

ASYMPTOTIC SILENCE-BREAKING SINGULARITIES

WOEI CHET LIM^{1*}, CLAES UGGLA^{2†} AND JOHN WAINWRIGHT^{3‡}

¹*Department of Mathematics and Statistics, Dalhousie University, Halifax, Nova Scotia, Canada B3H 3J5*

²*Department of Physics, University of Karlstad, S-651 88 Karlstad, Sweden*

³*Department of Applied Mathematics, University of Waterloo, Waterloo, Ontario, Canada N2L 3G1*

February 12, 2006

Abstract

We discuss three complementary aspects of scalar curvature singularities: asymptotic causal properties, asymptotic Ricci and Weyl curvature, and asymptotic spatial properties. We divide scalar curvature singularities into two classes: so-called asymptotically silent singularities and singularities that break asymptotic silence. The emphasis in this paper is on the latter class which have not been previously discussed. We illustrate the above aspects and concepts by describing the singularities of a number of representative explicit perfect fluid solutions.

PACS number(s): 04.20.-q, 98.80.Jk, 04.20.Dw, 04.20.Ha

gr-qc/0511139

1 Introduction

In a recent paper a general framework for locally analyzing Einstein's field equations (EFE) was presented [1]. As a first application the structure of generic spacelike singularities was investigated, and an attractor describing the asymptotic dynamical properties of such singularities was presented. The results in [1] were later numerically supported in [2] and [3]. In [4] isotropic singularities were investigated by extending the methods developed in [1] to also include the null geodesic equations. Gradually a picture about asymptotic causal structure has emerged, indicating that generic spacelike singularities and isotropic singularities are examples in which local null cones collapse onto a timeline towards the singularity, leading to the formation of particle horizons with a size that shrinks to zero (see p. 75 and Fig. 1 on p. 76 in [5]). Since the shrinking of horizons prevents communication, the phenomenon was referred to as *asymptotic silence* and a corresponding singularity as being asymptotically silent (see [3] for further discussion). However, for some solutions particle horizons may not form, or if they do form, they may not shrink to zero size. The best known example showing that the particle horizon can be broken in one spatial direction is a spatially homogeneous (SH), Bianchi type I dust solution, with a so-called weak null singularity (see [6] p. 176). The asymptotic behaviour of this solution towards the singularity gives one illustration of how *asymptotic silence-breaking* can occur.

Our goal in this paper is to illustrate the notion of asymptotic silence-breaking at a scalar curvature singularity by analyzing a selection of explicit perfect fluid solutions, thereby extending our understanding of the asymptotic causal structure of singularities. Although our examples

*Electronic address: wclim@mathstat.dal.ca

†Electronic address: claes.uggla@kau.se

‡Electronic address: jwainwri@math.uwaterloo.ca

are non-generic, we believe that they may be of importance for more general phenomena, worthy of further study. In this context it is worth pointing out that non-generic solutions can play an important role in determining the behaviour of generic solutions. For example, self-similar cosmological solutions, which are certainly non-generic, have been shown to play an important role in determining the dynamics of generic solutions.¹

The outline of the paper is as follows. In Sec. 2 we describe three complementary geometrical aspects of a matter singularity: firstly, according to its asymptotic causal properties in terms of asymptotic silence or asymptotic silence-breaking; secondly, according to its scalar Ricci and Weyl curvature; thirdly, according to how a spatial volume element is deformed towards the singularity. In Sec. 3 we give a number of selected examples that show how asymptotic silence can be broken and how this is connected with the above aspects. In Sec. 4 we conclude with some remarks about our results and their implications. A brief introduction to the orthonormal frame formalism and to Hubble-normalized variables is given in Appendix A. In Appendix B we give the non-tilted SH self-similar solutions, which describe the asymptotic behaviour of the examples in Sec. 3.

Although we make use of the orthonormal frame formalism (see, for example [7]) for doing the necessary calculations, a detailed knowledge of this formalism is not required in the main body of the paper.

2 Geometrical properties of singularities

In this paper we consider perfect fluid solutions of EFE with a barotropic equation of state $p = p(\rho)$, where p and ρ are the isotropic pressure and energy density in the rest frame of the fluid. Linear equations of state are characterized by the constant γ defined by $p = (\gamma - 1)\rho$. We assume that $\rho > 0$ and $0 < \gamma \leq 2$.

The solutions that we consider have a matter singularity, i.e. the matter density ρ diverges since the overall length scale ℓ tends to zero

$$\lim_{\ell \rightarrow 0} \rho = +\infty. \quad (1)$$

Our analysis of singularities relies heavily on the use of scale-invariant variables that are defined by normalizing with the appropriate power of the Hubble scalar H of the fluid congruence. The Hubble scalar is defined in terms of the 4-velocity \mathbf{u} of the perfect fluid by

$$H = \frac{1}{3} \nabla_a u^a, \quad (2)$$

and serves to define the length scale ℓ according to

$$H = \frac{\dot{\ell}}{\ell}, \quad (3)$$

where the overdot denotes differentiation along \mathbf{u} . Important dimensionless quantities related to H are the *deceleration parameter* q and the *spatial Hubble gradient* r_a , defined by

$$q = -\frac{\dot{H}}{H^2} - 1, \quad r_a = -\frac{h_a{}^b \nabla_b H}{H^2}. \quad (4)$$

where $h_a{}^b = \delta_a{}^b + u_a u^b$ projects into the 3-space orthogonal to \mathbf{u} .

We now introduce three complementary geometrical aspects of curvature singularities.

¹The Kasner solutions, which are self-similar, determine the past attractor for generic cosmological solutions (see [1]), while the flat FL solution, which is also self-similar, underlies the generic phenomenon of intermediate isotropization (see [11], p. 312).

2.1 Asymptotic causal singularity structure

The first aspect of singularities that we consider is the asymptotic causal properties towards the singularity. We define a part of a singularity to be asymptotically silent if all observers that approach it have particle horizons that shrink to zero size. If a particle horizon does not shrink to zero, or if a particle horizon does not form in one or more directions, we say that *asymptotic silence-breaking* occurs.

Reference [1] heuristically links the formation of shrinking particle horizons to the limit

$$\lim_{\ell \rightarrow 0} E_\alpha^i = 0 \quad (5)$$

([1], p. 103502-10) of the Hubble-normalized components of the spatial frame vector fields

$$E_\alpha^i = \frac{e_\alpha^i}{H} \quad (6)$$

(these vector fields are introduced in Appendix A). However, as we will see, it seems to be necessary to also demand that

$$\lim_{\ell \rightarrow 0} \dot{U}_\alpha = 0, \quad \lim_{\ell \rightarrow 0} r_\alpha = 0, \quad (7)$$

in order to provide sufficient conditions for asymptotic silence to hold. Here the r_α are the frame components of the spatial Hubble gradient (4), and the \dot{U}_α are the frame components of the Hubble-normalized acceleration of the fluid (see (117) and (121) in the Appendix).

Below we will show how asymptotic silence can be broken in various ways. We will give examples where

$$\lim_{\ell \rightarrow 0} E_\alpha^i = \text{diag}(\text{const}, 0, 0), \quad (8)$$

where $\text{const} \neq 0$ (if const appears in an asymptotic expression, it will from now on be assumed to be non-zero), leading to asymptotic silence-breaking in one direction only. We refer to such a singularity as *partially silent*. It is also possible that

$$\lim_{\ell \rightarrow 0} E_\alpha^i = C_\alpha^i, \quad (9)$$

where the constant 3×3 matrix C_α^i has higher rank than 1 (rank 1 yields equation (8)), which leads to the breaking of asymptotic silence in more than one direction, although we shall not consider examples with this property, apart from the Friedmann-Lemaître model to follow.² In addition we give examples of asymptotic silence-breaking when $\lim_{\ell \rightarrow 0} E_\alpha^i = \infty$ for some values of α and i , and when some of the components of E_α^i oscillate indefinitely as $\ell \rightarrow 0$, so that $\lim_{\ell \rightarrow 0} E_\alpha^i$ does not exist.

To illustrate some of the above let us consider the flat Friedmann-Lemaître model:

$$ds^2 = -dt^2 + t^{4/3\gamma} [dr^2 + r^2(d\theta^2 + \sin^2\theta d\phi^2)], \quad (10)$$

$$\rho = \frac{4}{3\gamma^2 t^2}, \quad p = (\gamma - 1)\rho, \quad \mathbf{u} = \partial/\partial t. \quad (11)$$

The radial null geodesics are given by

$$\left(\frac{dt}{dr}\right)^2 = t^{4/3\gamma}. \quad (12)$$

²Asymptotic silence-breaking in more than one direction appears to necessitate violation of an energy condition, i.e. $p < 0$ or even $\rho + 3p < 0$ (see (17) to follow).

Solving for $r = r(t)$ shows that the past light cone at $r = 0, t = t_0$ is generated by the following family of null geodesics;

$$r - b = \begin{cases} -\frac{3\gamma}{3\gamma-2} t^{(3\gamma-2)/3\gamma} & , & b = \frac{3\gamma}{3\gamma-2} t_0^{(3\gamma-2)/3\gamma} & , & \gamma \neq \frac{2}{3} \\ -\ln t & , & b = \ln t_0 & , & \gamma = \frac{2}{3} \end{cases} . \quad (13)$$

Observe that

$$\lim_{t \rightarrow 0^+} r = \begin{cases} b & , & \frac{2}{3} < \gamma \leq 2 \\ +\infty & , & 0 < \gamma \leq \frac{2}{3} \end{cases} . \quad (14)$$

It follows that if $\frac{2}{3} < \gamma \leq 2$, the past light cone intersects the hypersurface $t = 0$ at

$$r = r_h(t_0) = \frac{3\gamma}{3\gamma-2} t_0^{(3\gamma-2)/3\gamma} , \quad (15)$$

thereby creating a particle horizon, as shown in Fig. 1. Moreover, the horizon shrinks to zero size as the singularity is approached since $\lim_{t_0 \rightarrow 0} r_h = 0$, and thus asymptotic silence holds. However, if $\gamma \leq \frac{2}{3}$ no particle horizon is formed, see Fig. 1, and hence asymptotic silence is broken.

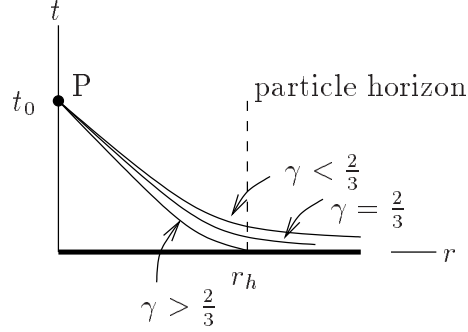


Figure 1: The past light cone of the point P and the initial singularity at $t = 0$, showing the particle horizon at $r = r_h$ in the case $\gamma > \frac{2}{3}$, and the absence of a particle horizon in the case $\gamma \leq \frac{2}{3}$.

In this example the Hubble-normalized spatial frame vectors are given by

$$E_\alpha^i = \frac{3\gamma}{2} t^{(3\gamma-2)/3\gamma} \text{diag}(1, 1, 1) , \quad (16)$$

so that

$$\lim_{t \rightarrow 0^+} E_\alpha^i = \begin{cases} \text{diag}(0, 0, 0) & , & \frac{2}{3} < \gamma \leq 2 \\ \text{diag}(1, 1, 1) & , & \gamma = \frac{2}{3} \\ \text{diag}(+\infty, +\infty, +\infty) & , & 0 < \gamma \leq \frac{2}{3} \end{cases} , \quad (17)$$

which shows that in this example the condition (5) is a reliable indicator of the existence of a particle horizon. This result is to be compared with the casual properties depicted in Fig. 1.

2.2 Asymptotic scalar curvature singularity structure

The second aspect of curvature singularities that is relevant to our discussion is the asymptotic behaviour of the Ricci and Weyl curvature scalars.

Firstly, it is of interest to consider the Hubble-normalized curvature scalars, the density parameter

$$\Omega = \frac{\rho}{3H^2}, \quad (18)$$

describing Hubble-normalized Ricci curvature (equivalently $R_{ab}R^{ab}/H^4$), and

$$\mathcal{C} := \frac{C_{abcd}C^{abcd}}{H^4}, \quad \mathcal{C}^* := \frac{C_{abcd}^*C^{abcd}}{H^4}, \quad (19)$$

i.e, the Hubble-normalized Weyl scalar and pseudoscalar invariants. If $\lim_{\ell \rightarrow 0} \Omega \neq 0$, then the Ricci scalar curvature, or equivalently, the matter content, is dynamically significant at the singularity and if $\lim_{\ell \rightarrow 0} \mathcal{C} \neq 0$ or $\lim_{\ell \rightarrow 0} \mathcal{C}^* \neq 0$, then the Weyl scalar curvature is dynamically significant at the singularity.

Secondly, it is of interest to consider the ratios

$$C_R := \frac{C_{abcd}C^{abcd}}{\rho^2}, \quad C_R^* := \frac{C_{abcd}^*C^{abcd}}{\rho^2} \quad (20)$$

(or equivalently $C_{abcd}C^{abcd}/R_{ab}R^{ab}$ and $C_{abcd}^*C^{abcd}/R_{ab}R^{ab}$), indicating the relative rates at which the Ricci and Weyl curvature scalars diverge. Note that

$$C_R = \frac{\mathcal{C}}{9\Omega^2}, \quad C_R^* = \frac{\mathcal{C}^*}{9\Omega^2}, \quad (21)$$

as follows from (18)–(20). We here introduce the following classification. A scalar curvature singularity is said to be

- Ricci-dominated if $\lim_{\ell \rightarrow 0} C_R = 0$ and $\lim_{\ell \rightarrow 0} C_R^* = 0$
- Weyl-Ricci balanced if C_R, C_R^* are bounded, and at least one of them has a non-zero limit, or oscillates indefinitely as $\ell \rightarrow 0$
- Weyl-dominated if one of C_R, C_R^* is unbounded, possibly oscillating

(see [8] for a similar classification used for discussing future asymptotes, although $C_{abcd}^*C^{abcd}$ was not considered in that paper).

As an example, consider an isotropic singularity (see e.g., [9], [4]). In this case the Hubble-normalized Ricci curvature is dynamically significant while the Hubble-normalized Weyl curvature is not,

$$\lim_{\ell \rightarrow 0} \Omega = 1, \quad \lim_{\ell \rightarrow 0} \mathcal{C} = 0, \quad \lim_{\ell \rightarrow 0} \mathcal{C}^* = 0. \quad (22)$$

This leads to $\lim_{\ell \rightarrow 0} C_R = 0$ and $\lim_{\ell \rightarrow 0} C_R^* = 0$, and one thus has asymptotic Ricci dominance. On the other hand, at a generalized Mixmaster singularity (see [1]), $\lim_{\ell \rightarrow 0} \Omega = 0$ while the Weyl curvature is dynamically significant, which yields asymptotic Weyl dominance. Indeed, $\lim_{\ell \rightarrow 0} \mathcal{C}$ and $\lim_{\ell \rightarrow 0} \mathcal{C}^*$ do not even exist, which implies that $\lim_{\ell \rightarrow 0} C_R$ and $\lim_{\ell \rightarrow 0} C_R^*$ do not exist either. The non-existence of these limits is due to the oscillating nature of the generalized Mixmaster dynamics. However, \mathcal{C} and \mathcal{C}^* are bounded (since they are bounded on the Kasner subset and the vacuum Bianchi type II subset which describe the attractor for Mixmaster dynamics, see [1]) and hence C and C^* exhibit bounded oscillations, while C_R and C_R^* oscillate in an unbounded manner.

2.3 Asymptotic spatial structure

In [11] (p. 30) a classification of matter singularities is given that reflects the change of shape of a spherical element of a fluid as a singularity is approached. This classification is based on the limiting behaviour of the scale factors ℓ_α in the eigendirections of the expansion tensor, and is applicable to models in which the limits of the scale factors exist or are infinite. In practice it is more convenient to base this classification on the Hubble-normalized expansion tensor (see e.g., [11] p. 19)

$$\Theta_{\alpha\beta} = \frac{\theta_{\alpha\beta}}{H}, \quad (23)$$

which is related to the Hubble-normalized shear tensor³ $\Sigma_{\alpha\beta}$ according to

$$\Theta_{\alpha\beta} = \delta_{\alpha\beta} + \Sigma_{\alpha\beta}. \quad (24)$$

It follows that $\Theta^\alpha_\alpha = 3$. We are considering models for which the limit $\Theta_{\alpha\beta}$ exists as the singularity is approached, say

$$\lim_{\ell \rightarrow 0} \Theta_{\alpha\beta} = \Theta_{\alpha\beta}^s, \quad (25)$$

where $\Theta_{\alpha\beta}^s$ is a 3×3 symmetric matrix, which in general depends on spatial position. We diagonalize $\Theta_{\alpha\beta}^s$, and let Θ_α^s denote its diagonal entries. If the limit of the deceleration parameter exists,

$$\lim_{\ell \rightarrow 0} q = q^s, \quad (26)$$

then one can define the *shape parameters* p_α according to

$$p_\alpha = \frac{\Theta_\alpha^s}{1 + q^s}, \quad \sum_{\alpha=1}^3 p_\alpha = \frac{3}{1 + q^s}, \quad (27)$$

which for the well-known Kasner solution become the so-called Kasner parameters. The exponents p_α are related to diagonalized limit values of $\Sigma_{\alpha\beta}$ by

$$\Sigma_\alpha^s = \frac{3p_\alpha}{\sum p_\alpha} - 1, \quad (28)$$

The classification (first introduced by Thorne [10] for Bianchi type I cosmologies) is based on the signs of the p_α :

- (i) $(+, +, +)$, point,
- (ii) $(+, +, 0)$, barrel,
- (iii) $(+, +, -)$, cigar,
- (iv) $(+, 0, 0)$, pancake,

and cycle on 1,2,3, cf. p. 121 [11]. Heuristically, if $\Theta_1^s > 0$ ($= 0, < 0$, respectively), for example, the length scale in the 1-direction will tend to zero at the singularity (respectively a *const*, $+\infty$), thereby justifying this terminology.

2.4 Asymptotically self-similar singularities

The simplest cosmological singularities are *asymptotically self-similar*, in the sense that the limits of all Hubble-normalized scalars exist as $\ell \rightarrow 0$, and equal the constant values of an exact self-similar SH solution, which we shall refer to as the *asymptotic solution at the singularity*. The examples in Section 3, except for the Szekeres and Wainwright-Marshman solutions in Sections 3.2.2 and 3.2.3, have an asymptotically self-similar singularity. The corresponding asymptotic solutions are as follows:

³ $\Sigma_{\alpha\beta}$ is defined by (117) in the Appendix.

- i) the Taub form of flat spacetime [11, p. 193],
- ii) the diagonal vacuum plane wave solution [11, p. 191],
- iii) the Collins VI_h perfect fluid solution [11, p. 190].

One can think of the Taub form of flat spacetime as the special Kasner vacuum solution for which the curvature tensor is zero. For brevity we shall refer to this form of flat spacetime as the *Taub solution*. Likewise we shall refer to ii) as the *plane wave solution*.

For any self-similar SH solution, the Hubble-normalized expansion tensor $\Theta_{\alpha\beta}$ has constant components, and the deceleration parameter q is constant. These quantities determine the shape parameters p_α according to (27). For the three above-mentioned solutions we have:

- i) The Taub solution:

$$(p_\alpha) = (1, 0, 0). \quad (29)$$

- ii) The plane wave solution:

$$(p_\alpha) = (1, r + \sqrt{r(1-r)}, r - \sqrt{r(1-r)}), \quad (30)$$

where r satisfies $0 < r < 1$. The p_α satisfy the conditions

$$p_1 + p_2 + p_3 = p_1^2 + p_2^2 + p_3^2 > 1. \quad (31)$$

- iii) The Collins VI_h solution:

$$(p_\alpha) = (1, \frac{2-\gamma+rs}{2\gamma}, \frac{2-\gamma-rs}{2\gamma}), \quad (32)$$

where $s^2 = (2-\gamma)(3\gamma-2)$, with $\frac{2}{3} < \gamma < 2$, and r satisfies $0 < r < 1$. The p_α satisfy the conditions

$$\frac{2}{\gamma} = p_1 + p_2 + p_3 > p_1^2 + p_2^2 + p_3^2. \quad (33)$$

The line element for the Taub solution is given by

$$ds^2 = -dt^2 + t^2 dx^2 + dy^2 + dz^2. \quad (34)$$

Full details about the solutions ii) and iii) are given in Appendix B. For a given cosmological solution with asymptotically self-similar singularity, one can identify the asymptotic solution by calculating the p_α .

3 Explicit examples

We divide our examples into two main categories: spatially homogeneous examples and inhomogeneous examples. The quantity $C_{abcd}^* C^{abcd}$, and thus C^* and C_R^* , is identically zero for all examples except for the Wainwright-Marshman solutions in Section 3.2.3. Hence these quantities will not be given except in this last case.

3.1 Spatially homogeneous examples

3.1.1 Bianchi type I perfect fluid solution

We consider the LRS Bianchi type I perfect fluid solution with a linear equation of state, given by ([11], p. 199 with $p_\alpha = (1, 0, 0)$):

$$ds^2 = -A^{2(\gamma-1)} dt^2 + t^2 A^{-\frac{2}{3}} dx^2 + A^{\frac{4}{3}} (dy^2 + dz^2), \quad (35)$$

where

$$A^{2-\gamma} = \alpha + m^2 t^{2-\gamma}. \quad (36)$$

The matter quantities are

$$\mathbf{u} = A^{-(\gamma-1)} \partial/\partial t, \quad \rho = \frac{4m^2}{3t^\gamma A^\gamma}, \quad p = (\gamma-1)\rho, \quad (37)$$

where α and m are two positive constants, and γ satisfies $0 < \gamma < 2$.

The Hubble scalar is given by

$$H = \frac{1}{3} A^{1-\gamma} t^{-1} [1 + A^{-(2-\gamma)} m^2 t^{2-\gamma}] \sim t^{-1} \rightarrow \infty, \quad (38)$$

and the Weyl scalar by

$$C_{abcd} C^{abcd} = \frac{64\alpha^2 m^4}{27A^4 t^{2\gamma}}. \quad (39)$$

There is a curvature singularity at $t = 0$, and the rates of growth of the curvature scalars are

$$\rho \sim t^{-\gamma} \rightarrow \infty, \quad C_{abcd} C^{abcd} \sim t^{-2\gamma} \rightarrow +\infty, \quad (40)$$

as follows from (37) and (39). The shape parameters are $p_\alpha = (1, 0, 0)$, which by (29) shows that the asymptotic solution at the singularity is the Taub solution. In addition it follows from Section 2.2 that the singularity is of the pancake type. Equations (38) and (40) imply that the density parameter and the Hubble-normalized Weyl scalar satisfy

$$\Omega \sim t^{2-\gamma} \rightarrow 0, \quad \mathcal{C} \sim t^{2(2-\gamma)} \rightarrow 0, \quad (41)$$

which is consistent with being asymptotic to the Taub solution. In addition, it follows from (37) and (39) that the ratio C_R , as defined by (20), satisfies

$$C_R \rightarrow \frac{4}{3}. \quad (42)$$

Equations (40)–(42) show that the singularity is Weyl-Ricci balanced, and is such that neither the Weyl nor the Ricci curvature is dynamically significant.

It follows from (35) and (38) that the Hubble-normalized frame components satisfy

$$E_\alpha^i \sim \text{diag}(\beta, t, t) \rightarrow (\beta, 0, 0), \quad (43)$$

where $\beta = 3\alpha^{\frac{3\gamma-2}{3(2-\gamma)}}$, showing asymptotic silence-breaking in the x -direction, and this is further confirmed by the form of past null cone of a typical point, as shown in Fig. 2 a).

The dust case is discussed extensively by Hawking and Ellis on p. 145-147 in [6]. By means of a coordinate transformation that takes the Taub line element, $-dt^2 + t^2 dx^2$, to explicit flat form $-dT^2 + dX^2$, they show that one can make a C^0 extension of the metric across a null surface where the above “interior” solution is joined with flat spacetime (see our Fig. 2b and Fig. 22 on p.146 in [6]). For this reason the singularity is referred to as a “weak null singularity”.

3.1.2 Bianchi type VI_h two-fluid solution

Wainwright [12] has given an exact SH perfect fluid solution of Bianchi type VI_h with a barotropic equation of state. For our purposes it is useful to consider a special case of this solution determined by setting $u = \frac{1}{10}, v = w = \frac{3}{10}$ in [12], in which case the group parameter is $h = -1/9$. In this case the matter content can be interpreted as two non-interacting dust and radiation fluids. The line-element is given by:

$$ds^2 = A^{-2} (-dt^2 + t^2 dx^2) + (t e^x)^{4/5} dy^2 + A^2 (t e^x)^{-2/5} dz^2, \quad (44)$$

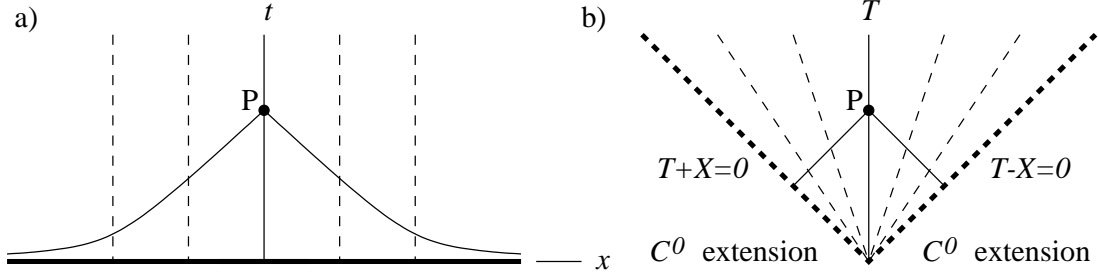


Figure 2: Figures a) and b) show the causal structure associated with the LRS Bianchi I solution that exhibits a weak null singularity, and illustrates asymptotic silence-breaking. It is an example in which no particle horizon forms in one direction, i.e., it is an example of a partially silent singularity. Fig. 2a) utilizes the present coordinates while Fig. 2b) uses coordinates adapted to the null structure of the singularity. In both figures the thin dashed lines represent the fluid worldlines.

where

$$A = \alpha_s + \alpha_m t^{2/5}. \quad (45)$$

The constants α_s, α_m are required to satisfy $\alpha_s > 0, \alpha_m > 0$. The matter quantities are given by

$$\mathbf{u} = A \partial / \partial t, \quad \rho = \rho_R + \rho_M, \quad p = \frac{1}{3} \rho_R, \quad (46)$$

where

$$\rho_R = \frac{12}{25} \alpha_s \alpha_m t^{-8/5}, \quad \rho_M = \frac{8}{25} \alpha_m^2 t^{-6/5}. \quad (47)$$

Note that asymptotically the equation of state is linear with a radiation equation of state, i.e. $\lim_{t \rightarrow 0} p/\rho = 1/3$.

The Hubble scalar is given by

$$H = \frac{2}{5} A t^{-1} \sim t^{-1} \rightarrow \infty, \quad (48)$$

and the Weyl scalar by

$$C_{abcd} C^{abcd} = -A^4 t^{-4} \left[2 \left(\frac{24}{25} \right)^2 T + O(T^2) \right], \quad (49)$$

where $T = t \partial_t \ln A \sim t^{2/5} \rightarrow 0$. There is a curvature singularity at $t = 0$, and the rates of growth of the curvature scalars are

$$\rho \sim t^{-8/5} \rightarrow \infty, \quad C_{abcd} C^{abcd} \sim -t^{-18/5} \rightarrow -\infty, \quad (50)$$

as follows from (46), (47) and (49). The shape parameters are given by

$$p_\alpha = \left(1, \frac{2}{5}, -\frac{1}{5} \right), \quad (51)$$

and satisfy (31), which shows that the asymptotic solution at the singularity is the plane wave solution with $h = -\frac{1}{9}$. In addition, it follows from Section 2.3 that the singularity is of the cigar type.

Equations (48) and (50) imply that the density parameter and the Hubble-normalized Weyl scalar satisfy

$$\Omega \sim t^{2/5} \rightarrow 0, \quad \mathcal{C} \sim -t^{2/5} \rightarrow 0, \quad (52)$$

which is consistent with being asymptotic to the plane wave solution. In addition, equation (50) shows that the ratio C_R satisfies

$$C_R \sim -t^{-2/5} \rightarrow -\infty. \quad (53)$$

which implies that the singularity is Weyl-dominated, in the terminology of Section 2.2.

It follows from (44) and (48) that the Hubble-normalized frame components satisfy

$$E_\alpha^i \sim \text{diag}(\text{const}, t^{3/5}, t^{6/5}) \rightarrow (\text{const}, 0, 0), \quad (54)$$

showing asymptotic silence-breaking in the x -direction.

It is instructive to introduce the same ‘‘Taub’’ coordinate transformation as was used in [6] to show that the previous LRS Bianchi type I solution was C^0 extendible. Let

$$\begin{cases} T + X = t e^x \\ T - X = t e^{-x} \end{cases} \Rightarrow \begin{cases} t = \sqrt{T^2 - X^2} \\ e^x = \sqrt{\frac{T+X}{T-X}} \end{cases}, \quad (55)$$

which leads to

$$ds^2 = A^{-2}(-dT^2 + dX^2) + (T+X)^{4/5} dy^2 + A^2 (T+X)^{-2/5} dz^2, \quad (56)$$

with $A = \alpha_s + \alpha_m (T^2 - X^2)^{1/5}$. The metric is C^0 on $T - X = 0$ where it can be joined with flat spacetime in the region $T - X < 0$, but not on $T + X = 0$. Thus this plane wave singularity is also (partially) a weak null singularity.

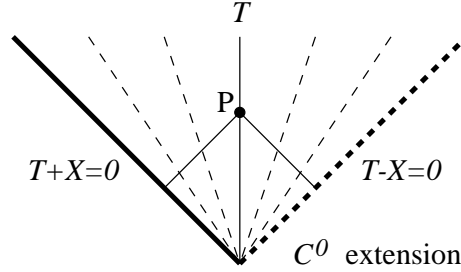


Figure 3: The causal structure associated with the Bianchi type VI_h two-fluid solution in T, X coordinates.

3.2 Inhomogeneous examples

3.2.1 Senovilla-Vera (1997) dust solution

Senovilla and Vera have presented a number of explicit dust solutions in [13]. One which is useful for our purposes is case (i) on p. 3483 in [13]. This solution can be written in fluid comoving coordinates so that the line-element takes the form:

$$ds^2 = -dt^2 + t^2 dx^2 + Y^2 dy^2 + (t e^{-x})^{1-k} dz^2, \quad (57)$$

where

$$Y = c_- (t e^{-x})^{b_-} + m^2 (t e^x)^b + c_+ (t e^{-x})^{b_+}, \quad (58)$$

$$b = \frac{1}{2}(1+k), \quad b_\pm = \frac{1}{2}(1 \pm \sqrt{2-k^2}), \quad -1 < k < 1. \quad (59)$$

The parameters b, b_{\pm} satisfy $b_- < 0 < b < 1 < b_+$. The matter quantities are given by

$$\mathbf{u} = \partial/\partial t, \quad \rho = \frac{(1-k^2)m^2(t e^x)^b}{t^2 Y}, \quad p = 0. \quad (60)$$

The Hubble scalar is given by

$$H = \frac{1}{6t} [3 - k + 2Y^{-1}[c_- b_- (t e^{-x})^{b_-} + m^2 b (t e^x)^b + c_+ b_+ (t e^{-x})^{b_+}]], \quad (61)$$

and there is a simple expression for the Weyl scalar:

$$C_{abcd}C^{abcd} = \rho^2 \left[\frac{4}{3} - \frac{2Y}{m^2 (t e^x)} \right]. \quad (62)$$

The solution yields three distinct types of singularity depending on the sign of c_- . For our purposes, however, it suffices to consider the cases $c_- > 0$ and $c_- = 0$.

Case i) $c_- > 0$

There is a curvature singularity at $t = 0$, and the rates of growth of the curvature scalars are

$$\rho \sim t^{-2+b-b_-} \rightarrow \infty, \quad C_{abcd}C^{abcd} \sim -t^{-4+b-b_-} \rightarrow -\infty, \quad (63)$$

as follows from (60) and (62). The shape parameters are given by

$$p_{\alpha} = (1, b_-, 1 - b). \quad (64)$$

It follows that the p_{α} satisfy (31), which shows that the asymptotic solution at the singularity is the diagonal plane wave solution, with $h = -[1 - \frac{1}{2}(k + \sqrt{2-k^2})]/[1 + \frac{1}{2}(k + \sqrt{2-k^2})]$. Since $b_- < 0 < b < 1$, the singularity is of the cigar type.

It follows from (61) and (63) that the density parameter and the Hubble-normalized Weyl scalar both tend to zero:

$$\Omega \sim t^{b-b_-} \rightarrow 0, \quad \mathcal{C} \sim -t^{b-b_-} \rightarrow 0, \quad (65)$$

as required for a solution that is asymptotic to the diagonal plane wave solution. In addition, equation (63) shows that the ratio C_R satisfies

$$C_R \sim -t^{-(b-b_-)} \rightarrow -\infty, \quad (66)$$

which implies that the singularity is Weyl-dominated.

This inhomogeneous solution is asymptotically homogeneous in the sense that the spatial Hubble gradient tends to zero:

$$r_1 \sim t^{b-b_-} \rightarrow 0. \quad (67)$$

It follows from (57) and (61) that the Hubble-normalized frame components have the following limit:

$$E_{\alpha}{}^i \sim \text{diag} \left(\frac{3}{2-b+b_-}, t^{b_+}, t^b \right) \rightarrow (\text{const}, 0, 0), \quad (68)$$

which suggests asymptotic silence-breaking in the x -direction, confirmed in Fig. 4.

Case ii) $c_- = 0$

There is a singularity at $t = 0$, with $Y = 0$ also, and the rates of growth of the curvature scalars are

$$\rho \sim t^{-2} \rightarrow \infty, \quad C_{abcd}C^{abcd} \sim -t^{-4} \rightarrow -\infty, \quad (69)$$

as follows from (60) and (62). The shape parameters are given by

$$p_\alpha = (1, \frac{1}{2}(1+k), \frac{1}{2}(1-k)). \quad (70)$$

It follows that the p_α are given by (32) with $\gamma = 1$ and $r = k$, which shows that the asymptotic solution at the singularity is the Collins VI_h solution. Since $-1 < k < 1$, the singularity is of the anisotropic point type.

It follows from (61) and (69) that the density parameter and the Hubble-normalized Weyl scalar have the following limits:

$$\Omega \rightarrow \frac{3}{4}(1-k^2), \quad C \rightarrow -\frac{27}{8}(1-k^2)^2, \quad (71)$$

as required for a solution that is asymptotic to the Collins VI_h solution for dust (set $\gamma = 1$, $r = k$ in (143) and (144)). In addition, equations (71) and (21) show that

$$C_R \rightarrow -\frac{2}{3}, \quad (72)$$

which implies that the singularity is Weyl-Ricci balanced.

This solution is also asymptotically homogeneous, since

$$r_1 \sim t^{b+^{-b}} \rightarrow 0. \quad (73)$$

It follows from (57) and (61) that the Hubble-normalized frame components have the following limit:

$$E_\alpha{}^i \sim \text{diag} \left(\frac{3}{2}, t^{(1-k)/2}, t^{(1+k)/2} \right) \rightarrow (\text{const}, 0, 0), \quad (74)$$

which shows asymptotic silence-breaking in the x -direction.

As in the SH cases it is instructive to make a ‘‘Taub’’ transformation of the coordinates (55). It turns out that the $c_- > 0$ case is C^0 extendible through $T + X = 0$, but not through $T - X = 0$ (the $c_- = 0$ case is not extendible) and thus the singularity in this case is (partially) a weak null singularity. See Fig. 4 for the causal structure of the singularity for the various cases. Asymptotic silence is broken in the x -direction and the singularity is partially silent for both cases.

3.2.2 Szekeres solution

The Szekeres solutions [14], [15] are a family of cosmological dust solutions. These solutions can be interpreted as exact perturbations of the Friedmann-Lemaître models, with both a growing and decaying mode. For our purposes it suffices to consider a special Szekeres model whose line-element is

$$ds^2 = -dt^2 + t^{4/3} (X^2 dx^2 + dy^2 + dz^2), \quad (75)$$

where

$$X = a + kx t^{-1}, \quad (76)$$

and a, k are positive constants. The matter quantities are given by

$$\mathbf{u} = \partial/\partial t, \quad \rho = \frac{4}{3} a t^{-2} X^{-1}, \quad p = 0. \quad (77)$$

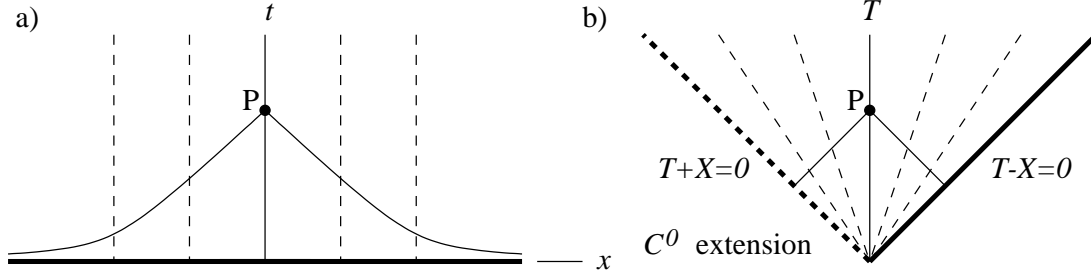


Figure 4: a) shows the causal structure associated with the Senovilla-Vera 1997 solution in both cases $c_- > 0$ and $c_- = 0$, in the original coordinates, while b) shows it for the $c_- > 0$ case in T, X coordinates.

The Hubble scalar is given by

$$H = \frac{2}{3t} \left[1 - \frac{kx}{2tX} \right], \quad (78)$$

and the Weyl scalar by

$$C_{abcd}C^{abcd} = \frac{4}{3}\rho^2 \left(1 - \frac{X}{a} \right)^2. \quad (79)$$

If $x < 0$ the singularity is determined by $X = 0$, and the rates of growth of the curvature scalars are

$$\rho \sim X^{-1} \rightarrow \infty, \quad C_{abcd}C^{abcd} \sim X^{-2} \rightarrow \infty, \quad (80)$$

as follows from (77) and (79). The shape parameters are $p_\alpha = (1, 0, 0)$, which shows that the singularity is of the pancake type.

It follows from (78) and (80) that the density parameter and the Hubble-normalized Weyl scalar satisfy

$$\Omega \sim X \rightarrow 0, \quad \mathcal{C} \sim X^2 \rightarrow 0, \quad (81)$$

and in addition, equations (77) and (79) show that

$$C_R \rightarrow \frac{4}{3}, \quad (82)$$

which implies that the singularity is Weyl-Ricci balanced.

The preceding results suggest that the solution is asymptotic to the Taub solution at the singularity. However, the behaviour of the spatial Hubble gradient r_α shows that the solution is not asymptotically spatially homogeneous. It follows from (78) and (121) that there is one non-zero component given by

$$r_1 = \frac{3kat^{4/3}}{X(kx - 2tX)^2}, \quad (83)$$

which implies that

$$r_1 \sim X^{-1} \rightarrow \infty. \quad (84)$$

It thus appears that the asymptotic state is not adequately described by the Taub solution. We shall refer to this singularity as being asymptotically ‘‘Taub-like’’.

It follows from (75) and (78) that the Hubble-normalized frame components satisfy

$$E_\alpha^i \rightarrow (f(x), 0, 0), \quad (85)$$

where $f(x)$ is a positive function, suggesting asymptotic silence-breaking in the x -direction.

The causal structure in this example is quite different than in the previous examples. Even though $E_1^1 \not\rightarrow 0$, a particle horizon does form for an observer with $x < 0$, and initially shrinks in size as $X \rightarrow 0^+$. However, the horizon does not shrink to zero size, as is confirmed by the numerical simulations that are shown in Fig. 5. Thus asymptotic silence is broken for the $x < 0$ part of the singularity.

This example also illustrates that the nature of the singularity can depend on the fluid worldline. If $x = 0$ a two-parameter set of fluid lines approach an asymptotically silent isotropic singularity (also known as an LK asymptote) [9], [4] characterized by $p_\alpha = \frac{2}{3}(1, 1, 1)$ and $\Omega \rightarrow 1$. If $x > 0$ the fluid lines approach an asymptotically silent singularity of the cigar type described by the LRS Kasner asymptote $p_\alpha = \frac{1}{3}(-1, 2, 2)$ (see Appendix B).

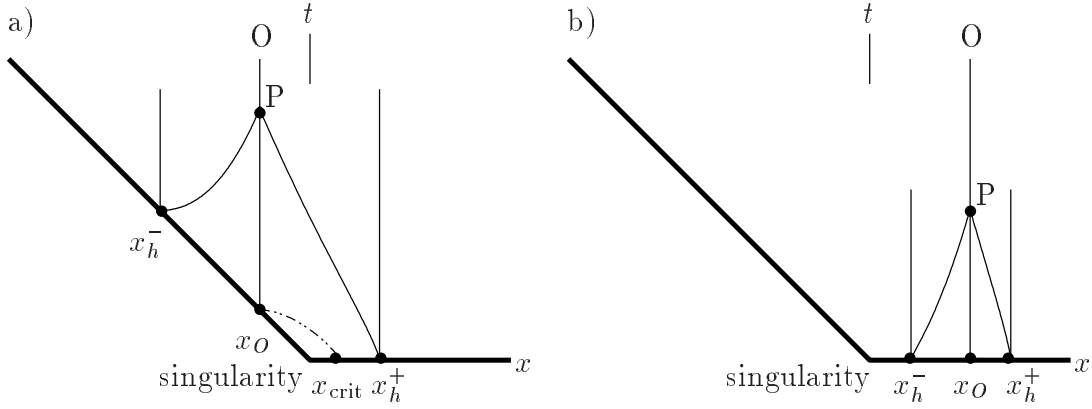


Figure 5: This figure shows the particle horizon at an event P for an observer O, generated numerically. The particle horizon is determined by the past null geodesics through P, which intersect the singularity at $x = x_h^+$ and $x = x_h^-$. In case a) the particle horizon does not shrink to zero since as P approaches the singularity, x_h^+ approaches x_{crit} , the value determined by the dotted null geodesic. In case b) the particle horizon does shrink to zero since $x_h^\pm \rightarrow x_O$ as P approaches the singularity.

As a result, the limits of Ω and \mathcal{C} at the singularity are position-dependent (i.e. depend on x). In particular $\Omega \rightarrow 0$ when $x \neq 0$ but $\Omega \rightarrow 1$ at $x = 0$, i.e. as the singularity is approached Ω develops a so-called spike (see also [16, pp 91–96]). In addition, $\mathcal{C} \rightarrow 0$ when $x \leq 0$ while $\mathcal{C} \rightarrow \text{const}$ when $x > 0$, i.e., \mathcal{C} asymptotically approaches a step function.

3.2.3 Wainwright-Marshman solutions

The stiff perfect fluid solution found by Wainwright and Marshman [18] can be written as

$$ds^2 = t^{2m} e^n (-dt^2 + dx^2) + t^{1/2} (dy + w dz)^2 + t^{3/2} dz^2, \quad (86)$$

$$\rho = p = (m + \frac{3}{16}) t^{-2(m+1)} e^{-n}, \quad \mathbf{u} = t^{-m} e^{-n/2} \partial/\partial t. \quad (87)$$

Here $w = w(t - x)$ is an arbitrary function, $n = n(t - x)$ is determined according to

$$n' = (w')^2, \quad (88)$$

and m is a constant that satisfies $m \geq -\frac{3}{16}$.

The Hubble scalar is given by

$$H = t^{-(m+1)} e^{-n/2} B, \quad (89)$$

where

$$B = \frac{1}{3} [(m+1) + \frac{1}{2} t (w')^2]. \quad (90)$$

The non-zero Hubble-normalized components of the spatial frame vectors are

$$E_1^1 = \frac{t}{B}, \quad E_A^I = \frac{t^{m+\frac{1}{4}} e^{n/2}}{B} \begin{pmatrix} t^{1/2} & 0 \\ -w & 1 \end{pmatrix}. \quad (91)$$

The Hubble-normalized kinematic quantities are

$$\Sigma_{11} = 2 - \frac{1}{B}, \quad \Sigma_{22} = \frac{1}{4B} - 1, \quad \Sigma_{33} = \frac{3}{4B} - 1, \quad \Sigma_{23} = \frac{t^{1/2} w'}{2B}, \quad \dot{U}_1 = -\frac{t (w')^2}{2B}. \quad (92)$$

Finally the deceleration parameter and the non-zero component of the spatial Hubble gradient are

$$q = -1 + \frac{m+1}{B} - \frac{t (w')^2}{6B^2} - r_1, \quad r_1 = -\frac{t (w')^2}{2B} + \frac{t^2 w' w''}{3B^2}. \quad (93)$$

The Weyl tensor can best be described by giving the complex Newman-Penrose scalars [19]

$$\psi_0 = -\frac{1}{4} m t^{-(m+1)} e^{-n}, \quad (94)$$

$$\psi_2 = \frac{1}{8} \left[\frac{4}{3} (m - \frac{3}{8}) + i w' t^{1/2} \right] t^{-(m+1)} e^{-n}, \quad (95)$$

$$\psi_4 = \left[-\frac{1}{4} m + \frac{3}{4} (w')^2 t + i (w'' - (w')^3 - m w' t^{-1}) t^{3/2} \right] t^{-(m+1)} e^{-n} \quad (96)$$

(see [22], p. 3037 for these formulae). The Weyl curvature scalars are then given by

$$C_{abcd} C^{abcd} - i C_{abcd}^* C^{abcd} = 16 (3\psi_2^2 - 4\psi_1 \psi_3 + \psi_0 \psi_4). \quad (97)$$

We choose the arbitrary function $w(t-x)$ so that $n(t-x)$ satisfies

$$\lim_{t-x \rightarrow 0^+} n(t-x) = -\infty. \quad (98)$$

The spacetime region is then defined by the inequalities

$$t > 0, \quad t - x > 0. \quad (99)$$

Fluid worldlines with $x \leq 0$ encounter a curvature singularity at $t = 0$ and those with $x > 0$, at $t = x$, since $\rho \rightarrow \infty$ in both cases, as follows from (87). In other words, the given initial singularity has two branches that depends on the sign of x , namely $t = 0, x \leq 0$ and $t = x, x > 0$, respectively.

At the $t = 0, x \leq 0$ part of the singularity the solution satisfies

$$\lim_{t \rightarrow 0^+} r_1 = 0 = \lim_{t \rightarrow 0^+} \dot{U}_1, \quad \lim_{t \rightarrow 0^+} (\Sigma_{\alpha\beta}) = \frac{1}{m+1} \text{diag} (2m-1, -\frac{1}{4} (4m+1), \frac{1}{4} (5-4m)), \quad (100)$$

which implies that the shape parameters p_α are given by

$$p_\alpha = \frac{1}{m+1} (m, \frac{1}{4}, \frac{3}{4}), \quad (101)$$

and satisfy (131). The solution is thus asymptotic to a Jacobs stiff fluid solution. The singularity type is: cigar ($-\frac{3}{16} < m < 0$), barrel ($m = 0$), or anisotropic point ($m > 0$). We also have

$$\lim_{t \rightarrow 0^+} E_\alpha^i = 0, \quad (102)$$

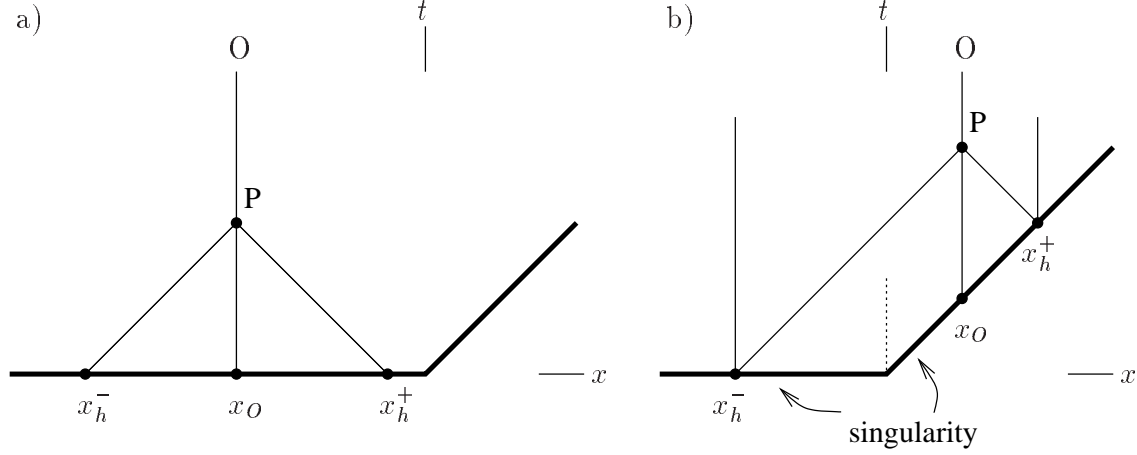


Figure 6: The figure shows the causal structure associated with the Wainwright-Marshman solution. The left part of the singularity is asymptotically silent and is described asymptotically by the Jacobs stiff fluid solution. The right part of the singularity breaks asymptotic silence.

and so we expect that the singularity is asymptotically silent, which is confirmed by Fig. 6a).

The nature of the $t - x = 0, x > 0$ part of the singularity depends on the behaviour of the arbitrary function $w(t - x)$ or $n(t - x)$. However, since the null geodesics in the tx -space are given by $t \pm x = \text{const}$, the causal structure in the tx -space is independent of the nature of the behaviour of $w(t - x)$ or $n(t - x)$. Observe that the particle horizons of observers approaching the part of the singularity given by $t - x = 0, x > 0$ do not shrink to zero size as the singularity is approached. Hence asymptotic silence is broken. Even though the causal structure is unaffected, the curvature properties depend significantly on the choice of $w(t - x)$ and $n(t - x)$.

There are two possibilities that are compatible with equation (98):

- (i) $\lim_{t \rightarrow x^+} n'(t - x) = +\infty$
- (ii) $n'(t - x)$ oscillates and is unbounded as $t \rightarrow x^+$.

Case (i): $\lim_{t \rightarrow x^+} n'(t - x) = +\infty$

It follows that

$$\lim_{t \rightarrow x^+} B = +\infty \quad (\text{recall } n' = (w')^2), \quad (103)$$

which in turn implies

$$\lim_{t \rightarrow x^+} \Sigma_{\alpha\beta} = \text{diag}(2, -1, -1), \quad \lim_{t \rightarrow x^+} q = 2. \quad (104)$$

It follows that the shape parameters are $p_\alpha = (1, 0, 0)$, suggesting that the solution is asymptotic to the Taub solution. But equations (92) and (93) imply that⁴

$$\lim_{t \rightarrow x^+} r_1 = \lim_{t \rightarrow x^+} \dot{U}_1 = -3, \quad (105)$$

⁴Here we make the additional assumption that $\lim_{t \rightarrow x^+} n''(t - x)/[n'(t - x)]^2 = 0$, which will be satisfied if, for example, $n(t - x) = -C(t - x)^{-b}$, where b and C are positive constants.

so that the asymptotic state is inhomogeneous. It thus appears that the asymptotic state is not adequately described by the Taub solution. We shall refer to this singularity as being asymptotically “Taub-like” (See Section 3.2.2).

In addition, we have the following asymptotic expressions:

$$H \sim e^{-n/2}(w')^2 \rightarrow \infty, \quad (106)$$

$$\rho \sim e^{-n} \rightarrow \infty, \quad C_{abcd}C^{abcd} \sim e^{-2n}(w')^2 \rightarrow \infty, \quad (107)$$

$$\Omega \sim (w')^{-4} \rightarrow 0, \quad \mathcal{C} \sim (w')^{-6} \rightarrow 0, \quad (108)$$

$$C_R \sim (w')^2 \rightarrow \infty. \quad (109)$$

This part of the singularity is thus a Weyl-dominated scalar curvature singularity. Although it is “Taub-like” as regards the shape parameters, the curvature ratio C_R does not have the same limit at the singularity as in the solution that is asymptotic to the Taub solution (see equation (42)). It is also worth noting that $\Omega \rightarrow 0$, which shows that this solution is not in the generic class of stiff fluid solutions which satisfy $\Omega \not\rightarrow 0$, and whose behaviour near the singularity was analyzed by Andersson and Rendall [20].

Even though $E_\alpha^i \rightarrow 0$ as the singularity is approached, asymptotic silence is still broken, because the particle horizon to the left of an observer with $x > 0$ does not shrink to zero at the singularity, i.e. x_h^- does not tend to x_O in Fig. 6b). Thus this example shows that $E_\alpha^i \rightarrow 0$ *does not necessarily lead to horizons that shrink to zero*. This example thus forces us to make a distinction between $E_\alpha^i \rightarrow 0$ and particle horizons that shrink to zero. Since asymptotic silence should reflect an invariant physical causal property we therefore choose to define asymptotic silence as horizons shrinking to zero, cf. [3]. However, it should be pointed out that although the solution approaches the so-called silent boundary (see [1] and [3]), it approaches a part not described by SH equations (see [1] and [21] for a discussion about the equations on the silent boundary) since $\dot{U}_\alpha, r_\alpha \neq 0$. It is likely that this affects the relationship between E_α^i and the causal structure.

Case (ii): $n'(t-x)$ oscillates and is unbounded as $t \rightarrow x^+$

Let us consider the following possible choice [22]:

$$w'(t-x) = \frac{\alpha}{t-x} \sin\left(\frac{b}{t-x}\right), \quad t-x > 0 \quad \Rightarrow \quad (110)$$

$$n(t-x) = -\frac{\alpha^2}{2(t-x)} + \frac{\alpha^2}{4b} \sin\left(\frac{2b}{t-x}\right) \quad (111)$$

(so that $\lim_{t \rightarrow x^+} n = -\infty$, as required in equation (98)). This yields

- $\lim_{t \rightarrow x^+} E_A^I = 0$ ($A, I = 2, 3$), while $\lim_{t \rightarrow x^+} E_1^1$ does not exist, since E_1^1 oscillate while remaining bounded. It follows that the singularity is non-silent.
- Ω oscillates and is bounded.
- $\lim_{t \rightarrow x^+} \Sigma_{\alpha\beta}$ does not exist because of (bounded) oscillations.
- \mathcal{C} oscillates and is bounded but \mathcal{C}^* oscillates and is *unbounded* (due to w'').

It is perhaps natural to refer to this kind of singularity as being strongly Weyl-dominated, i.e. *the Hubble-normalized Weyl curvature is unbounded*.⁵ This solution is thus a counterexample to

⁵This behaviour at the singularity is reminiscent of the future evolution of Bianchi type VII₀ models (see [23]).

Solution	asymptotic solution	asymptotic spatial structure	$\lim_{\ell \rightarrow 0} C_R$	$\lim_{\ell \rightarrow 0} q$
LRS Bianchi type I	Taub	pancake	$\frac{4}{3}$	2
Bianchi type VI _h two-fluid	plane wave ($h = -\frac{1}{9}$)	cigar	$-\infty$	$\frac{3}{2}$
SV (1997) dust $c_- > 0$	plane wave ($-1 < h < 0$)	cigar	$-\infty$	$\frac{2}{1-3h}$
SV (1997) dust $c_- = 0$	Collins VI _h ($-1 < h < 0$)	point	$-\frac{2}{3}$	$\frac{1}{2}$
Szekeres	Taub-like	pancake	$\frac{4}{3}$	2

Table 1: Summary of properties of the diagonal solutions that exhibit asymptotic silence-breaking at the singularity.

the hope that the Hubble-normalized Weyl curvature is bounded at any cosmological singularity. It is nevertheless possible that the Hubble-normalized Weyl scalars are bounded at asymptotically silent singularities.

4 Concluding remarks

In this paper we have presented a collection of cosmological solutions that illustrate the phenomenon of asymptotic silence-breaking. The examples, apart from the Szekeres and Wainwright-Marshman solutions, are asymptotically self-similar at the singularity, in the sense that the limits of all Hubble-normalized variables exist as $\ell \rightarrow 0$, and equal the constant values of an exact self-similar SH solution. The properties of the singularities of these solutions are summarized in Table 1.

We comment on a number of common features of these examples:

- i) All of the solutions have a Ricci and a Weyl curvature scalar singularity in the sense that

$$\lim_{\ell \rightarrow 0} \rho = \infty, \quad \lim_{\ell \rightarrow 0} C_{abcd} C^{abcd} = \pm\infty. \quad (112)$$

- ii) Asymptotic silence-breaking occurs in one direction only.

On the other hand, the differences are found in:

- i) The Hubble-normalized Weyl curvature components and scalars, and the density parameter:

Taub	$\mathcal{E}_{\alpha\beta} \ \& \ \mathcal{H}_{\alpha\beta} \rightarrow 0$	$\mathcal{C} \rightarrow 0$	$\Omega \rightarrow 0$
Plane wave	$\mathcal{E}_{\alpha\beta} \ \& \ \mathcal{H}_{\alpha\beta} \not\rightarrow 0$	$\mathcal{C} \rightarrow 0$	$\Omega \rightarrow 0$
Collins VI _h	$\mathcal{E}_{\alpha\beta} \ \& \ \mathcal{H}_{\alpha\beta} \not\rightarrow 0$	$\mathcal{C} \not\rightarrow 0$	$\Omega \not\rightarrow 0$

The variables $\mathcal{E}_{\alpha\beta}$ and $\mathcal{H}_{\alpha\beta}$ are Hubble-normalized frame components of the electric and magnetic parts of the Weyl tensor as defined in Appendix A, equation (118).

- ii) Asymptotic spatial structure (see Table 1)

iii) Weyl-Ricci balance, as described by the ratio C_R (see Table 1)

It is of interest to ask what statements can be made in general about solutions that are asymptotic to the Taub solution, the plane wave solution and the Collins VI_h solution at the singularity. On the basis of the properties of the asymptotic solutions in Appendix B, we can draw the following conclusions:

- In any perfect fluid solution asymptotic to the Taub solution at the singularity, asymptotic silence-breaking occurs with rank $(E_\alpha^i) = 1$, for any γ , $0 < \gamma < 2$. The spatial singularity type is pancake. We are unable to predict whether $\lim_{\ell \rightarrow 0} C_R = \frac{4}{3}$ in general, since the ratio C_R is undefined for the Taub solution. A detailed analysis of the asymptotic behaviour would be needed to answer this question.
- In any SH perfect fluid solution asymptotic to the plane wave solution at the singularity, if $1 \leq \gamma < 2$ then asymptotic silence-breaking occurs with rank $(E_\alpha^i) = 1$, and the singularity is of the cigar type. The group parameter h will satisfy $-1 < h < 0$. We are unable to predict whether $\lim_{\ell \rightarrow 0} C_R = -\infty$ in general (if $\gamma \geq 1$) since the ratio C_R is undefined for the plane wave solution. A detailed analysis of the asymptotic behaviour would be needed to answer this question.
- In any perfect fluid solution asymptotic to the Collins VI_h solution at the singularity, if $1 \leq \gamma < 2$ then asymptotic silence-breaking occurs with rank $(E_\alpha^i) = 1$. The group parameter h will satisfy $-1 \leq h < 0$. The spatial singularity type is point, barrel or cigar, and is necessarily a point if $\gamma = 1$. We can also predict that if $\gamma = 1$, the limit of the curvature ratio C_R will be $-\frac{2}{3}$. If $1 < \gamma < 2$, the limit will also be non-zero, but its value will depend on γ and h through equations (143) and (144).

The remaining examples, the Szekeres solutions and the Wainwright-Marshman solutions (case ii)), are not asymptotically self-similar at the asymptotically silence-breaking part of the singularity. In the Szekeres solution, asymptotic self-similarity fails because $\lim_{\ell \rightarrow 0^+} r_1 = +\infty$, while the behaviour of the Hubble-normalized curvature scalars (Ω , \mathcal{C} and C_R) is the same as the solutions that are asymptotic to the Taub solution. For this reason we refer to the Szekeres solution as being ‘‘Taub-like’’ at the singularity. In the Wainwright-Marshman solutions of class ii), the failure of asymptotic self-similarity is reflected in the curvature, in the sense that the limits of the Hubble-normalized energy density and Weyl tensor as $\ell \rightarrow 0$ do not exist. Indeed, \mathcal{C}^* is even *unbounded*. They also constitute an interesting example of asymptotic silence-breaking, since E_1^1 oscillates so that the limit of this quantity does not exist.

The Wainwright-Marshman solutions that belong to class (i) exhibit asymptotic silence-breaking even though $E_\alpha^i \rightarrow 0$. In this solution, however, r_α, \dot{U}_α have non-zero limits. This raises the question: are the conditions $\lim_{\ell \rightarrow 0} (E_\alpha^i, r_\alpha, \dot{U}_\alpha) = (0, 0, 0)$, given by equations (5) and (7), sufficient for asymptotic silence,⁶ i.e., the existence of particle horizons that shrink to zero as the singularity is approached?

Acknowledgement

WCL and CU gratefully acknowledge the Isaac Newton Institute For Mathematical Sciences at the University of Cambridge where part of this work was done. CU is supported by the Swedish Research Council. JW is supported by the Natural Sciences and Engineering Research Council of Canada.

⁶They are not necessary conditions since recurring spike formation (see [3]) provides a counterexample; in this case, asymptotic silence holds, with $\lim_{\ell \rightarrow 0} E_\alpha^i = 0$, but $\lim_{\ell \rightarrow 0} r_\alpha$ and $\lim_{\ell \rightarrow 0} \dot{U}_\alpha$ do not exist.

A Orthonormal frame formalism and Hubble-normalized variables

In this paper we use the orthonormal frame formalism in conjunction with Hubble-normalized variables to calculate the properties of the explicit solutions. We introduce an orthonormal frame $\{\mathbf{e}_0, \mathbf{e}_\alpha\}$, where $\mathbf{e}_0 = \mathbf{u}$, the 4-velocity of the perfect fluid, which is assumed to be irrotational. Local coordinates t, x^i are introduced such that

$$\mathbf{e}_0 = N^{-1}\partial_t, \quad \mathbf{e}_\alpha = e_\alpha^i \partial_i, \quad (113)$$

where ∂_t, ∂_i denote partial derivatives with respect to t and x^i ($\alpha = 1, 2, 3, i = 1, 2, 3$).

The commutators are decomposed according to:

$$[\mathbf{e}_0, \mathbf{e}_\alpha](f) = \dot{u}_\alpha \mathbf{e}_0(f) - [H\delta_\alpha^\beta + \sigma_\alpha^\beta + \epsilon_\alpha^\beta{}_\gamma \Omega^\gamma] \mathbf{e}_\beta(f) \quad (114)$$

$$[\mathbf{e}_\alpha, \mathbf{e}_\beta](f) = (2a_{[\alpha} \delta_{\beta]}^\gamma + \epsilon_{\alpha\beta\delta} n^{\delta\gamma}) \mathbf{e}_\gamma(f). \quad (115)$$

Here H is the Hubble scalar, \dot{u}^α the acceleration, $\sigma_{\alpha\beta}$ the tracefree shear, Ω^α describes the angular velocity of the spatial frame $\{\mathbf{e}_\alpha\}$ relative to a frame that is Fermi-propagated along the integral curves of \mathbf{e}_0 , while a^α and $n_{\alpha\beta} = n_{(\alpha\beta)}$ determine a spatial connection. Scale-invariant (dimensionless) Hubble-normalized variables are defined as follows (see [1]; for a slightly different set of definitions based on conformal considerations, see [24]):

$$\boldsymbol{\partial}_0 := \frac{\mathbf{e}_0}{H} = \mathcal{N}^{-1} \partial_t, \quad \boldsymbol{\partial}_\alpha := \frac{\mathbf{e}_\alpha}{H} = E_\alpha^i \partial_i, \quad \mathcal{N} := NH, \quad E_\alpha^i := \frac{e_\alpha^i}{H}, \quad (116)$$

$$\{\dot{U}^\alpha, \Sigma_{\alpha\beta}, A^\alpha, N_{\alpha\beta}, R^\alpha\} := \{\dot{u}^\alpha, \sigma_{\alpha\beta}, a^\alpha, n_{\alpha\beta}, \Omega^\alpha\}/H. \quad (117)$$

It is convenient to express the Weyl tensor in terms of its electric and magnetic parts, relative to the timelike congruence \mathbf{e}_0 , denoted by $E_{\alpha\beta}$ and $H_{\alpha\beta}$ (see [11], p. 19). Their Hubble-normalized components are defined by

$$(\mathcal{E}_{\alpha\beta}, \mathcal{H}_{\alpha\beta}) = (E_{\alpha\beta}, H_{\alpha\beta})/(3H^2). \quad (118)$$

The Weyl scalars introduced in Section 2.2 are expressed in terms of $E_{\alpha\beta}$ and $H_{\alpha\beta}$ as follows:

$$C_{abcd}C^{abcd} = 8(E_{\alpha\beta}E^{\alpha\beta} - H_{\alpha\beta}H^{\alpha\beta}), \quad C_{abcd}^*C^{abcd} = 16E_{\alpha\beta}H^{\alpha\beta}. \quad (119)$$

It follows from (19) and (118) that the Hubble-normalized Weyl scalars are given by

$$\mathcal{C} = 72(\mathcal{E}_{\alpha\beta}\mathcal{E}^{\alpha\beta} - \mathcal{H}_{\alpha\beta}\mathcal{H}^{\alpha\beta}), \quad \mathcal{C}^* = 144\mathcal{E}_{\alpha\beta}\mathcal{H}^{\alpha\beta}. \quad (120)$$

We note that the components $E_{\alpha\beta}, H_{\alpha\beta}$ can be calculated using the orthonormal frame formulae in [11] (p 35). Similar formulae for the Hubble-normalized components $\mathcal{E}_{\alpha\beta}, \mathcal{H}_{\alpha\beta}$ are given in [1] (p 21).

In terms of the orthonormal frame formalism, the deceleration parameter q and the frame components of the spatial Hubble gradient r_α , defined by (4), are given by

$$\boldsymbol{\partial}_0 H = -(q+1)H, \quad \boldsymbol{\partial}_\alpha H = -r_\alpha H, \quad (121)$$

It follows from Raychaudhuri's equation (see [1]) that

$$q = 2\Sigma^2 + \frac{1}{2}(3\gamma - 2)\Omega - \frac{1}{3}(\boldsymbol{\partial}_\alpha - r_\alpha + \dot{U}_\alpha - 2A_\alpha)\dot{U}^\alpha, \quad (122)$$

where $\Sigma^2 = \frac{1}{6}\Sigma_{\alpha\beta}\Sigma^{\alpha\beta}$. The SH spacetimes are characterized by $\boldsymbol{\partial}_\alpha(\) = 0$ for all Hubble-normalized variables, and $r_\alpha = 0 = \dot{U}_\alpha$, with the \mathbf{e}_α being tangential to the SH symmetry surfaces.

B The asymptotic solutions

The asymptotic solutions that were introduced in Section 2.4 are non-tilted SH self-similar solutions with perfect fluid source. A complete list of these solutions (line-element and matter variables) is given in [11] (Section 9.1). In this Appendix we give the Hubble-normalized variables for the specific solutions that are used in this paper, which are the ones with diagonal line-element. Since the line-elements are diagonal, one can introduce an orthonormal frame in a natural way. For the line-element

$$ds^2 = -N^2 dt^2 + X^2 dx^2 + Y^2 dy^2 + Z^2 dz^2 \quad (123)$$

we choose

$$e_0 = N^{-1} \partial_t, \quad e_1 = X^{-1} \partial_x, \quad e_2 = Y^{-1} \partial_y, \quad e_3 = Z^{-1} \partial_z, \quad (124)$$

so that the non-zero components e_α^i of the spatial frame vectors are

$$e_1^1 = X^{-1}, \quad e_2^2 = Y^{-1}, \quad e_3^3 = Z^{-1}. \quad (125)$$

The self-similar solutions in question are either of Bianchi type I or type VI_h .

B.1 Bianchi type I solutions

The line-element is [11, p. 187]

$$ds^2 = -dt^2 + t^{2p_1} dx^2 + t^{2p_2} dy^2 + t^{2p_3} dz^2. \quad (126)$$

The Hubble scalar and deceleration parameter are

$$H = b^{-1} t^{-1}, \quad q = b - 1, \quad b = \frac{3}{p_1 + p_2 + p_3}, \quad (127)$$

and the only non-zero Hubble-normalized commutation functions are the diagonal shear components,

$$\Sigma_{\alpha\alpha} = bp_\alpha - 1 \quad (\text{no sum}). \quad (128)$$

The constants p_α are the shape parameters (see (28)).

(1) *Flat Friedmann-Lemaître solution*

$$p_1 = p_2 = p_3 = \frac{2}{3\gamma}. \quad (129)$$

The matter density is given by

$$\rho = \frac{4}{3\gamma^2} t^{-2}, \quad 0 < \gamma \leq 2, \quad (130)$$

which implies that the density parameter is $\Omega = 1$. The Weyl tensor C_{abcd} is identically zero.

(2) *Kasner vacuum solutions and Jacobs stiff perfect fluid solutions*

$$p_1 + p_2 + p_3 = 1, \quad p_1^2 + p_2^2 + p_3^2 \begin{cases} = 1 & \text{for Kasner vacuum solutions,} \\ < 1 & \text{for Jacobs stiff fluid solutions.} \end{cases} \quad (131)$$

The non-zero Hubble-normalized Weyl tensor components are

$$\mathcal{E}_{11} = 2p_2 p_3 - p_1(p_2 + p_3). \quad (132)$$

where $\mathcal{E}_{\alpha\beta} = \text{diag}(\mathcal{E}_{11}, \mathcal{E}_{22}, \mathcal{E}_{33})$ and where $\mathcal{E}_{22}, \mathcal{E}_{33}$, are obtained from \mathcal{E}_{11} by cyclically permuting 1, 2, 3, and the density parameter is

$$\Omega = \frac{3}{2}(1 - p_1^2 - p_2^2 - p_3^2). \quad (133)$$

The choice $(p_\alpha) = (1, 0, 0)$, and cycle, yields the Taub form of flat spacetime.

B.2 Diagonal Bianchi type VI solutions

The line-element is [11, p. 190]

$$ds^2 = -dt^2 + t^2 dx^2 + t^{2p_2} e^{2c_2 x} dy^2 + t^{2p_3} e^{2c_3 x} dz^2. \quad (134)$$

The Hubble scalar and deceleration parameter are

$$H = b^{-1} t^{-1}, \quad q = b - 1, \quad b = \frac{3}{1+p_2+p_3}, \quad (135)$$

and the non-zero Hubble-normalized commutation functions are

$$\Sigma_{\alpha\beta} = \text{diag}(b-1, bp_2-1, bp_3-1), \quad A_1 = -\frac{b}{2}(c_2+c_3), \quad N_{23} = -\frac{b}{2}(c_2-c_3). \quad (136)$$

The constants $p_1 = 1$, p_2 , p_3 are thus the shape parameters (see (28)). The Hubble-normalized frame components are given by

$$E_1^1 = b, \quad E_2^2 = bt^{1-p_2} e^{-c_2 x}, \quad E_3^3 = bt^{1-p_3} e^{-c_3 x}. \quad (137)$$

The non-zero Hubble-normalized Weyl tensor components are

$$\mathcal{E}_{\alpha\beta} = \text{diag}(\alpha, -\frac{1}{2}\alpha + \beta, -\frac{1}{2}\alpha - \beta), \quad \mathcal{H}_{23} = \frac{1}{12} b^2 [(c_2+c_3)(p_2-p_3) - (c_2-c_3)(2-p_2-p_3)], \quad (138)$$

where

$$\alpha = \frac{1}{18} b^2 [(c_2-c_3)^2 - (p_2-p_3)^2], \quad \beta = \frac{1}{12} b^2 [(c_2^2 - c_3^2) - (p_2-p_3)(2-p_2-p_3)]. \quad (139)$$

(1) *Collins Bianchi type VI_h perfect fluid solution*

$$p_{2,3} = \frac{2-\gamma \pm rs}{2\gamma}, \quad c_{2,3} = \frac{(2-\gamma)r \pm s}{2\gamma}, \quad s = \sqrt{(2-\gamma)(3\gamma-2)}. \quad (140)$$

The parameter r determines the group parameter h according to

$$r^2 = r_c^2(-h), \quad r_c = \sqrt{(3\gamma-2)/(2-\gamma)}, \quad 0 \leq r < 1. \quad (141)$$

The matter quantities are given by

$$\rho = \frac{(2-\gamma)(1-r^2)}{\gamma^2} t^{-2}, \quad \frac{2}{3} < \gamma < \frac{2(1-h)}{1-3h}, \quad (142)$$

which implies, using (135), that

$$\Omega = \frac{3}{4}(2-\gamma)(1-r^2). \quad (143)$$

The Hubble-normalized Weyl scalar is given by

$$\mathcal{C} = -\frac{27}{8} s^2 (1-r^2) [(4-3\gamma)(2-\gamma)(1-r^2) + 12\gamma(\gamma-1)], \quad (144)$$

as follows from (138) and (120).

The spatial singularity type depends on γ and h . We restrict to non-negative pressure ($\gamma \geq 1$) which implies via (141) that $r_c^2 \geq 1$ and hence that $-h \leq r^2$. On writing the shape parameters p_2 and p_3 in the form

$$p_{2,3} = \frac{2-\gamma}{2\gamma} (1 \pm r_c r) \quad (145)$$

parameter range	p_α	spatial singularity type	restriction on γ
$rr_c < 1$	(+, +, +)	anisotropic point	$1 \leq \gamma < 2$
$rr_c = 1$	(+, +, 0)	barrel	$1 < \gamma < 2$
$rr_c > 1$	(+, +, -)	cigar	$1 < \gamma < 2$

Table 2: Classification of the singularity in the Collins Bianchi type VI_h perfect fluid solution with $\gamma \geq 1$. The value $\gamma = 1$ corresponds to $r_c = 1$.

using (140) and (141), we arrive at the classification shown in Table 2. It follows from (137) that in all cases,

$$\lim_{t \rightarrow 0} E_\alpha^i = \text{diag}(\text{const}, 0, 0). \quad (146)$$

(2) *Diagonal vacuum plane wave solution*

$$p_{2,3} = c_{2,3} = r \pm \sqrt{r(1-r)}, \quad (147)$$

where r is related to the group parameter h through

$$h = -\frac{r}{1-r}. \quad (148)$$

The Hubble-normalized quantities are given by

$$\Sigma_{11} = \frac{2(1-r)}{1+2r}, \quad \Sigma_{22,33} = b p_{2,3} - 1, \quad N_{23} = -b \sqrt{r(1-r)}, \quad A_1 = -br. \quad (149)$$

The non-zero Weyl tensor components are

$$\mathcal{E}_{22} = -\mathcal{E}_{33} = \mathcal{H}_{23} = \frac{1}{3}b^2(2r-1)\sqrt{r(1-r)}, \quad (150)$$

showing that the Weyl scalars (19), as given by (120), are zero.

The spatial singularity type depends on h (or equivalently r). The parameter r is in turn restricted by the value of the equation of state parameter γ of any non-tilted perfect fluid SH solution that is past asymptotic to the plane wave solution, according to

$$\gamma < \frac{2}{1+2r} \quad (151)$$

(see [26, p. 663]). We restrict to $\gamma \geq 1$, which implies that $0 \leq r < \frac{1}{2}$ (since $r \geq \frac{1}{2}$ implies $\gamma < 1$). It follows from (147) that $p_2 > 0$ and $p_3 < 0$, so that the singularity is of the cigar type. It also follows from (137) that

$$\lim_{t \rightarrow 0} E_\alpha^i = \text{diag}(\text{const}, 0, 0). \quad (152)$$

References

- [1] C. Ugla, H. van Elst, J. Wainwright, and G. F. R. Ellis, Past attractor in inhomogeneous cosmology, Phys. Rev. D **68**, 103502-1 (2003).
- [2] D. Garfinkle, Numerical simulation of generic singularities, Phys. Rev. Lett. **93**, 161101 (2004).

- [3] L. Andersson, H. van Elst, W. C. Lim, and C. Uggla, Asymptotic silence of generic cosmological singularities. *Phys. Rev. Lett.* **94**, 051101 (2005).
- [4] W. C. Lim, H. van Elst, C. Uggla, and J. Wainwright, Asymptotic isotropization in inhomogeneous cosmology, *Phys. Rev. D* **69**, 103507-1 (2004).
- [5] H. van Elst, C. Uggla, and J. Wainwright, Dynamical systems approach to G_2 cosmology, *Class. Quantum Grav.* **19**, 51 (2002).
- [6] S. W. Hawking, and G. F. R. Ellis, *The Large Scale Structure of Space-Time* (Cambridge, England, Cambridge University Press, 1973).
- [7] G. F. R. Ellis and H. van Elst, Cosmological models (Cargèse lectures 1998) in *Theoretical and Observational Cosmology*, edited by M. Lachièze-Rey, (Kluwer, Dordrecht), p. 1 (1999). (gr-qc/9812046)
- [8] J. D. Barrow and S. Hervik, The Weyl tensor in spatially homogeneous cosmological models, *Class. Quantum Grav.* **19**, 5173 (2002).
- [9] S. W. Goode and J. Wainwright, Isotropic singularities in cosmological models, *Class. Quantum Grav.* **2**, 99 (1985).
- [10] K. S. Thorne, Primordial element formation, primordial magnetic fields, and the isotropy of the universe, *Astrophys. J.* **148**, 51 (1967).
- [11] J. Wainwright and G. F. R. Ellis (Eds.), *Dynamical Systems in Cosmology* (Cambridge University Press, Cambridge, 1997).
- [12] J. Wainwright, A spatially homogeneous cosmological model with plane-wave singularity, *Phys. Lett.* **99A**, 301 (1983)
- [13] J. M. M. Senovilla and R. Vera, Dust G_2 cosmological models, *Class. Quantum Grav.* **14**, 3481 (1997).
- [14] P. Szekeres, A class of inhomogeneous cosmological models, *Comm. Math. Phys.* **41**, 55 (1979).
- [15] S. W. Goode, and J. Wainwright, Singularities and evolution of the Szekeres cosmological models, *Phys. Rev. D* **26**, 3315 (1982).
- [16] W. C. Lim, The dynamics of inhomogeneous cosmology, PhD Thesis, University of Waterloo, (2004). gr-qc/0410126.
- [17] J. M. M. Senovilla and R. Vera, Cylindrically symmetric dust spacetime, *Class. Quantum Grav.* **17**, 2843 (2000).
- [18] J. Wainwright and B. J. Marshman, Some exact cosmological models with gravitational waves, *Phys. Lett. A* **72**, 275 (1979).
- [19] E. T. Newman and R. Penrose, An approach to gravitational radiation by a method of spin coefficients, *J. Math. Phys.* **3**, 566 (1962).
- [20] L. Andersson and A. D. Rendall, Quiescent cosmological singularities, *Commun. Math. Phys.* **218** 479 (2001).
- [21] L. Andersson, H. van Elst, and C. Uggla, Gowdy phenomenology in scale-invariant variables, *Class. Quantum Grav.* **21**, S29 (2004).

- [22] J. Wainwright, An oscillatory big-bang singularity, *Can. J. Phys.* **64**, 200 (1986).
- [23] J. Wainwright, M. J. Hancock, and C. Uggla, Asymptotic self-similarity breaking at late times in cosmology, *Class. Quantum Grav.* **16**, 2577 (1999).
- [24] N. Röhr and C. Uggla, Conformal regularization of Einstein's field equations, *Class. Quantum Grav.* **22**, 3775 (2005).
- [25] J. Wainwright and L. Hsu, A dynamical systems approach to Bianchi cosmologies: orthogonal models of class A, *Class. Quantum Grav.* **6**, 1409 (1989).
- [26] J. Wainwright, Power law singularities in orthogonally spatially homogeneous cosmologies, *Gen. Rel. Grav.* **16**, 657 (1984).